

Anal Bioanal Chem (2006) 386:1587–1602  
DOI 10.1007/s00216-006-0795-5

ORIGINAL PAPER

# Labeling the human skeleton with $^{41}\text{Ca}$ to assess changes in bone calcium metabolism

E. Denk · D. Hillegonds · J. Vogel · A. Synal ·  
C. Geppert · K. Wendt · K. Fattinger · C. Hennessy ·  
M. Berglund · R. F. Hurrell · T. Walczyk

Received: 24 March 2006 / Revised: 18 August 2006 / Accepted: 22 August 2006 / Published online: 11 October 2006  
© Springer-Verlag 2006

**Abstract** Bone research is limited by the methods available for detecting changes in bone metabolism. While dual X-ray absorptiometry is rather insensitive, biochemical markers are subject to significant intra-individual variation. In the study presented here, we evaluated the isotopic labeling of bone using  $^{41}\text{Ca}$ , a long-lived radiotracer, as an alternative approach. After successful labeling of the skeleton, changes in the systematics of urinary  $^{41}\text{Ca}$  excretion are expected to directly reflect changes in bone

Ca metabolism. A minute amount of  $^{41}\text{Ca}$  (100 nCi) was administered orally to 22 postmenopausal women. Kinetics of tracer excretion were assessed by monitoring changes in urinary  $^{41}\text{Ca}/^{40}\text{Ca}$  isotope ratios up to 700 days post-dosing using accelerator mass spectrometry and resonance ionization mass spectrometry. Isotopic labeling of the skeleton was evaluated by two different approaches: (i) urinary  $^{41}\text{Ca}$  data were fitted to an established function consisting of an exponential term and a power law term for each individual; (ii)  $^{41}\text{Ca}$  data were analyzed by population pharmacokinetic (NONMEM) analysis to identify a compartmental model that describes urinary  $^{41}\text{Ca}$  tracer kinetics. A linear three-compartment model with a central compartment and two sequential peripheral compartments was found to best fit the  $^{41}\text{Ca}$  data. Fits based on the use of the combined exponential/power law function describing urinary tracer excretion showed substantially higher deviations between predicted and measured values than fits based on the compartmental modeling approach. By establishing the urinary  $^{41}\text{Ca}$  excretion pattern using data points up to day 500 and extrapolating these curves up to day 700, it was found that the calculated  $^{41}\text{Ca}/^{40}\text{Ca}$  isotope ratios in urine were significantly lower than the observed  $^{41}\text{Ca}/^{40}\text{Ca}$  isotope ratios for both techniques. Compartmental analysis can overcome this limitation. By identifying relative changes in transfer rates between compartments in response to an intervention, inaccuracies in the underlying model cancel out. Changes in tracer distribution between compartments were modeled based on identified kinetic parameters. While changes in bone formation and resorption can, in principle, be assessed by monitoring urinary  $^{41}\text{Ca}$  excretion over the first few weeks post-dosing, assessment of an intervention effect is more reliable ~150 days post-dosing when excreted tracer originates mainly from bone.

E. Denk · R. F. Hurrell · T. Walczyk (✉)  
Laboratory of Human Nutrition,  
Institute of Food Science and Nutrition, ETH Zurich,  
Schmelzbergstraße 7 (LFV D19.3),  
8092 Zürich, Switzerland  
e-mail: thomas.walczyk@ilw.agrl.ethz.ch

D. Hillegonds · J. Vogel  
Center for Accelerator Mass Spectrometry,  
Lawrence Livermore National Laboratory,  
Livermore, CA 94551-0808, USA

A. Synal  
Laboratory of Particle Physics,  
Paul Scherrer Institute/ETH Zurich,  
8092 Zürich, Switzerland

C. Geppert · K. Wendt  
Institute of Physics, Johannes Gutenberg University,  
55099 Mainz, Germany

K. Fattinger  
Department of General Internal Medicine, Inselspital,  
University Hospital Bern,  
3010 Bern, Switzerland

C. Hennessy · M. Berglund  
European Commission Joint Research Centre,  
Institute for Reference Materials and Measurements (IRMM),  
2440 Geel, Belgium

**Keywords**  $^{41}\text{Ca}$  · AMS · RIMS · Osteoporosis · Kinetic analysis · Compartmental modeling

## Introduction

Age-related osteoporosis has become a major public health concern due to the mean increase in life expectancy of three years per decade over the last century, a trend that seems set to continue [1]. With increasing age, bone balance becomes increasingly negative and bone becomes brittle [2]. The elderly face a significant increase in fracture risk, particularly of the spine, hip and wrist. Apart from a serious negative effect on individual welfare, the financial costs of osteoporosis are enormous. Annual total direct hospital costs arising from hip fractures alone amounted to nearly four billion euros within the European Union in 1996, and costs are expected to rise significantly [3].

A more detailed understanding of Ca metabolism in bone would help to better define the diet and life-style strategies needed for osteoporosis prevention. At present, no methodologies exist that allow the measurement of small changes in bone metabolism directly, with high sensitivity and on a short-term scale. Such small short-term changes in bone metabolism can result from alterations in diet and lifestyle. These changes accumulate with time and may play a significant role in maintaining bone health.

Alterations in bone Ca metabolism can be followed by monitoring changes in bone mineral density (BMD) with dual energy X-ray absorptiometry (DXA). The precision of conventional DXA machines is on the order of 1–2%, depending on the site measured [4, 5]. This limits the potential of DXA for the evaluation of the small changes in bone metabolism that can be expected from nutritional interventions and life-style changes. Changes in bone metabolism can also be monitored indirectly using biochemical markers of bone metabolism. Bone resorption can be assessed by measuring bone collagen degradation products in urine, while bone accretion can be monitored by measuring bone-specific proteins or enzymes in blood [6]. These biomarkers, however, are subject to strong intra-individual variations. Typical within-subject variations in biomarker concentration are on the order of 10–45% for bone resorption markers in urine and 5–10% for bone formation markers in serum [7], thus limiting the sensitivity of these tests. In addition, biomarkers of bone resorption and accretion are independent measures and cannot be combined to assess bone balance.

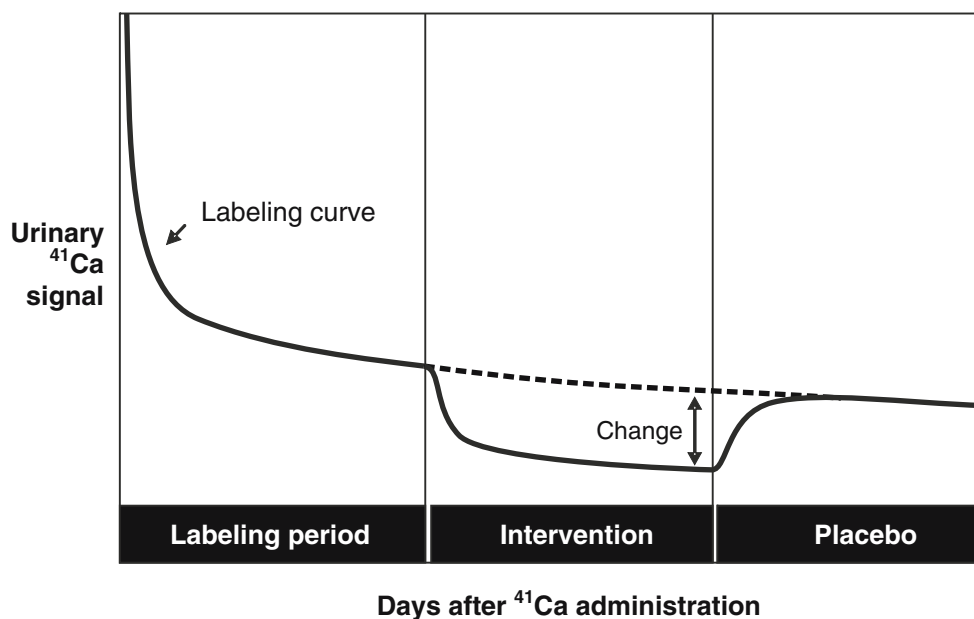
Isotopic techniques could overcome the current limitations of the existing techniques for monitoring bone metabolism. Changes in skeletal Ca metabolism can be determined directly by Ca kinetic studies involving oral and

intravenous administration of stable or radioactive Ca isotopes and by monitoring tracer appearance and disappearance in blood, urine and feces over 10–15 days. Although this technique reveals changes in bone accretion and resorption rates in response to an intervention, it is invasive and costly and difficult to apply to large subject groups. As Ca turnover in bone is slow, bone Ca can be labeled *in vivo* by administering Ca isotope tracers. Following administration, tracer not incorporated into the bone matrix is gradually excreted from the body in urine. After the excess tracer in the dosing compartment has been eliminated, the tracer in urine originates mainly from Ca incorporated into bone, and changes in bone metabolism can thus be assessed via the observed changes in urinary tracer excretion. However, the costs of bone labeling would be prohibitively high using stable Ca isotope labels, and it is not possible to use conventional Ca radiotracers because of ethical considerations about radiating the bone marrow. A potent alternative is  $^{41}\text{Ca}$ , a virtually stable, very long-lived radioisotope (half-life: 104,000 years) which can be detected at the ultratrace level using accelerator mass spectrometry (AMS) [8] or by resonance ionization mass spectrometry (RIMS) [9]. Conventional mass spectrometric techniques such as thermal ionization mass spectrometry (TIMS) or inductively coupled plasma mass spectrometry (ICP-MS) are not sensitive enough for this purpose. Even for high-resolution instruments, the abundance sensitivity is much too low to effectively suppress contributions to the  $^{41}\text{Ca}$  signal by neighboring peaks. Doses would have to be increased substantially to overcome limits on abundance sensitivity. This would jeopardize the main advantage of using  $^{41}\text{Ca}$  as a tracer, which is still a radioisotope despite its long half-life. Bone can be labeled at negligible health risk using AMS or RIMS for  $^{41}\text{Ca}$  analysis, because only minute amounts of the tracer have to be administered.

The feasibility of using  $^{41}\text{Ca}$  in bone research has been demonstrated by Johnson and coworkers, who labeled the skeleton of a single human subject with  $^{41}\text{Ca}$  and followed urinary  $^{41}\text{Ca}$  excretion over more than a year using AMS [10]. Also, in a human study, it was demonstrated more recently that the urinary  $^{41}\text{Ca}$  signal changes in response to bisphosphonate administration, a potent drug known to inhibit bone resorption [11]. Most recently, the serum  $^{41}\text{Ca}/^{40}\text{Ca}$  signal demonstrated significant differences between four healthy individuals and four end-stage renal failure patients [12].

When assessing changes in bone Ca metabolism in response to an intervention, the kinetics of urinary  $^{41}\text{Ca}$  excretion first need to be established for the individual. The Ca excretion pattern can be described mathematically using nonlinear curve-fitting techniques [13]. This so-called labeling curve can serve as a fixed index from which changes due to the intervention can be assessed (see Fig. 1).

**Fig. 1** Basic principle behind the use of  $^{41}\text{Ca}$  to monitor changes in bone metabolism. After administration of the isotope, the urinary excretion pattern of the tracer is followed during the labeling period. This so-called *labeling curve* serves as an unchanging index from which perturbations due to interventions can be assessed once steady-state kinetics for  $^{41}\text{Ca}$  are established, i.e. when all of the  $^{41}\text{Ca}$  that is recovered in urine was previously incorporated into bone



The effect of an intervention can be evaluated by calculating the change in the tracer signal during the intervention relative to the extrapolation from the labeling curve. In addition, compartmental modeling techniques can be applied for data evaluation. Techniques applied to study short-term Ca kinetics in humans closely follow well-established concepts [14]. It was demonstrated in an earlier experiment that the kinetics of  $^{41}\text{Ca}$  in the human body can be described by applying compartmental modeling techniques [10]. In our studies, a compartmental model that describes the observed  $^{41}\text{Ca}$  excretion pattern in urine was established via pharmacokinetic modeling techniques. By fitting the proposed model to observed data by nonlinear mixed-effects regression analysis, the effect of an intervention can be identified in the form of changes to the transfer rates of  $^{41}\text{Ca}$  between different Ca compartments.

Earlier experiments in human subjects have shown that, in principle, Ca in the human skeleton can be labeled using  $^{41}\text{Ca}$ , and that changes in bone Ca metabolism can be assessed to a much higher sensitivity than by any established technique. To make use of this technique in biomedical research, however, kinetics of urinary  $^{41}\text{Ca}$  excretion must be firmly established and evaluated, taking into account variations between subjects. The aim of the present study was to demonstrate the feasibility of using  $^{41}\text{Ca}$  to isotopically label bone and to describe mathematically the urinary excretion pattern of the  $^{41}\text{Ca}$  tracer after a single oral administration. We therefore administered  $^{41}\text{Ca}$  to 25 postmenopausal women and followed urinary  $^{41}\text{Ca}$  excretion at regular intervals for up to two years by AMS and RIMS. An integral part of this study was the production (by the EC Joint Research Centre, Institute for Reference Materials and Measurements; IRMM) of a standardized

dose material (IRMM-3703) and a set of certified  $^{41}\text{Ca}$  isotopic reference materials (IRMM-3701) for calibrating the various techniques used for  $^{41}\text{Ca}$  analysis against each other [15]. Tracer excretion was evaluated by nonlinear curve fitting and compartmental modeling techniques, including the identification of the most suitable model for describing long-term kinetics of  $^{41}\text{Ca}$  elimination in humans. Concepts for data collection and evaluation in human studies are proposed that may serve as the basis for further applications of this promising new technique.

## Experimental

### Subjects

Twenty-five apparently healthy women, at least five years postmenopausal, were recruited from a program for elderly citizens at the University of Zurich, Switzerland, and through advertisements in a local newspaper. All subjects were of Caucasian descent. None of the subjects had any known systemic disease or were taking any medication or dietary supplements that could potentially influence Ca homeostasis or bone status, including Ca, vitamin D, bisphosphonates, estrogens and diuretics. In order to exclude subjects with osteoporosis, a bone mineral density (BMD) scan was performed by DXA (Hologic QDR-4500A, Hologic Inc., Bedford, MA, USA) at a local hospital. Dietary Ca intake was assessed at the beginning of the study by a standardized food frequency questionnaire adapted for Swiss products and evaluated using the Swiss food composition database. The study protocol was approved by the Ethical Committee of the Swiss Federal

Institute of Technology, Zurich. Subjects were informed orally and in writing. Written informed consent was obtained from all volunteers. Subjects were asked to refrain from any medication that could potentially affect bone or cartilage metabolism and from the intake of vitamin and mineral supplements during the entire study. Compliance was monitored by regular interviews.

#### Study protocol

Subjects received a single oral dose of 3.7 kBq (100 nCi;  $2.823 \times 10^{-5}$  mmol)  $^{41}\text{Ca}$  as an aqueous solution together with a standardized light breakfast (toast, butter and jam) after an overnight fast on day 1 of the study. The drink consisted of 300.0 ml ultrapure (18 M $\Omega$ ) water to which the  $^{41}\text{Ca}$  solution had been added (2.00 ml). No food or fluids were allowed for three hours after test meal intake. Excretion of  $^{41}\text{Ca}$  was monitored in 24 h urine collections to establish the kinetics of urinary clearance for the isotopic label. Urine samples were collected at two, four, six and eight weeks after isotope administration, and then at monthly intervals for up to two years. Urine was collected in preweighed 2 L polyethylene bottles containing 10 ml 1 M  $\text{HNO}_3$  (p.a.) in order to minimize precipitation during storage. The weights of the  $\text{HNO}_3$  plus 24 h urine collections were recorded. At an average Ca amount of ~300 mg per 24 h urine collection, sampling blanks were negligible. In order to avoid seasonal variations in vitamin D status, subjects were supplemented throughout the entire study with 10  $\mu\text{g}$  vitamin D (Dekristol, 10  $\mu\text{g}$  cholecalciferol per capsule, Jenapharm AG, Jena, Germany) per day, commencing on the day of  $^{41}\text{Ca}$  administration. Compliance was monitored via self-reported intake and cross-checked by pill counts every month. Diet was unrestricted but subjects were requested to maintain their dietary habits or lifestyle, in particular their physical activity, over the course of the entire study.

#### $^{41}\text{Ca}$ dose material

The  $^{41}\text{Ca}$  source material used in this work was produced about 20 years ago at Oak Ridge National Laboratory (ORNL, Oak Ridge, TN, USA) by neutron activation of stable  $^{40}\text{Ca}$  (CaO), which was enriched to >99.998%, for three years. The activated material was run through an electromagnetic isotope separation (EMIS) process for  $^{41}\text{Ca}$  enrichment. Enrichment of the source material was 1.33% at the time of production [15]. A solution of this material with a nominal  $^{41}\text{Ca}/^{40}\text{Ca}$  ratio of 1% was made available to IRMM by Argonne National Laboratory (ANL, Argonne, IL, USA) and Purdue Rare Isotope Measurement Laboratory (West Lafayette, IN, USA). Production and certification of the isotopic reference materials and the dose

material at IRMM followed the requirements set out in ISO Guide 35 and are described in detail by [15]. The solution was first monitored at high sensitivity for gamma-ray emitting impurities using underground gamma-ray spectrometry in a 225 m-deep laboratory [16], and a certificate was issued. No significant radiocontaminants were found. It was then purified by precipitation of Ni as nickel NiS, and the purified solution, to be used as a dose material, was labeled IRMM-3703. Concentration levels of other metal impurities are available from IRMM [17].

An aliquot of 1.5 g of IRMM-3703 was gravimetrically diluted with a solution of high-purity HCl and aliquots, labeled IM-6010, were stored in sealed quartz ampoules. IM-6010 and IRMM-3703 were certified for Ca isotopic composition and IM-6010 was certified for Ca amount content by isotope dilution mass spectrometry on IM-6010, using a  $^{44}\text{Ca}$ -enriched isotopic reference material (IM-6009) as spike and the natural Ca reference material IM-6008 for k-factor determination. Isotope ratio measurements were performed using a double-filament technique on a modified single-sector Finnigan-MAT 260 thermal ionization mass spectrometer (TIMS, Finnigan MAT, Bremen, Germany). Measured  $^{41}\text{Ca}/^{40}\text{Ca}$  isotope ratios were corrected for residual  $^{41}\text{K}$  by applying a factor based on the  $^{39}\text{K}/^{40}\text{K}$  ratio measured during the same scan. Table 1 shows the certified isotopic composition of the dose material IRMM-3703.

#### Separation of Ca from urine for isotopic analysis

Ca was separated from collected urines for  $^{41}\text{Ca}$  analysis by oxalate precipitation at the Human Nutrition Laboratory, ETH Zurich, using established procedures [18]. One aliquot of 30.0 ml was taken from each 24-h urine sample. Separated calcium was analyzed at least in duplicate for  $^{41}\text{Ca}$  by AMS or RIMS. For Ca separation, sample pH was adjusted to 10 by addition of ammonium hydroxide and 60 ml of a saturated aqueous ammonium oxalate solution were added. Samples were heated to 70 °C followed by immersion into an ice bath for 90 min. Precipitates were separated by centrifugation and the supernatant was

**Table 1** Isotopic composition of the  $^{41}\text{Ca}$  dose material, IRMM-3703

Isotopic ratio	Certified value
$^{41}\text{Ca}/^{40}\text{Ca}$	0.012789(58)
$^{42}\text{Ca}/^{40}\text{Ca}$	0.0037979(96)
$^{43}\text{Ca}/^{40}\text{Ca}$	0.000390(11)
$^{44}\text{Ca}/^{40}\text{Ca}$	0.005750(18)
$^{46}\text{Ca}/^{40}\text{Ca}$	0.0000135(21)
$^{48}\text{Ca}/^{40}\text{Ca}$	0.0005268(80)

Uncertainties are given as expanded uncertainties ( $k=2$ ) and apply to the last two digits of the value.

removed. Precipitates were washed twice with 40 ml of saturated ammonium oxalate solution, followed by centrifugation and removal of the supernatant. To remove K and Na impurities, the precipitate was washed with 40 ml of a 0.1% (w/v) ammonium oxalate solution. In addition, Ca solutions were purified by ion exchange chromatography (AG50W-X8, Bio-Rad Laboratories, Hercules, CA, USA) using disposable columns. Purified solutions were transferred to a quartz beaker, covered with a quartz lid and dried overnight at 90 °C in an oven. Dried precipitates were ashed for 1 h in a muffle furnace at 1000 °C to remove traces of organic matter by which the Ca oxalate could be transformed into CaO. Ca recovery was >95% for the overall process. Ca separation was carried out following the principles of trace element analysis in order to reduce the risk of sample contamination. Only chemicals of analytical grade quality and ultrapure water (18 M $\Omega$ ) was used. Acids were purified by subboiling distillation. Labware was acid-washed and samples were handled under laminar flow conditions under constant separation blank monitoring.

#### Isotopic analysis

$n(^{41}\text{Ca})/n(^{40}\text{Ca})$  isotope amount ratios (hereafter referred to as  $^{41}\text{Ca}/^{40}\text{Ca}$  isotope ratios) were monitored in the collected urine samples up to 700 days after isotope administration. Due to restricted access to the AMS and RIMS machines, subjects were organized into four subgroups (A, B, C, D), which differed in the length of the monitoring period, the number of urine samples collected and analyzed and the analytical facilities used. The six subjects of subgroup A collected urine samples for ~700 days, and urine samples were analyzed for  $^{41}\text{Ca}$  at 20–30 time points per subject by AMS at Lawrence Livermore National Laboratory. Urinary  $^{41}\text{Ca}/^{40}\text{Ca}$  isotope ratios were monitored in subgroup B ( $n=4$ ) over a period of ~400 days at 10–12 time points. Urine samples from this subgroup from the early phase of the study (<150 d after tracer administration) were analyzed by RIMS at the University of Mainz, while samples from the later phase (>150 days after tracer administration) were analyzed by AMS at ETH Zurich. For the eight subjects in subgroup C, urinary  $^{41}\text{Ca}/^{40}\text{Ca}$  isotope ratios were determined at 7–8 time points covering a period of up to 260 days after isotope administration by AMS at ETH Zurich. For the three subjects in subgroup D,  $^{41}\text{Ca}/^{40}\text{Ca}$  isotope ratios were determined by AMS at ETH Zurich in 2–3 selected urine samples which were collected over a period of about 240 days (see Table 3).

#### $^{41}\text{Ca}$ isotopic analysis by AMS (ETH Zurich)

Ca separated from urine delivered as CaO (~10 mg Ca per sample) was converted to  $\text{CaH}_2$  as the target material for

AMS analysis. Isolated CaO was mixed with Zr and heated under high vacuum by electron bombardment and distilled to transform the sample into Ca metal [19]. Typical distillation yields were on the order of 85%. Ca metal was converted into its hydride by heating the metal under a hydrogen atmosphere at ~640 °C (hydration yield: 70–100%). The hygroscopic  $\text{CaH}_2$  samples obtained were pressed into Cu cathodes and stored under vacuum until the AMS measurement.

Samples were analyzed for  $^{41}\text{Ca}$  using the PSI/ETH 6 MV tandem AMS facility. The experimental set-up is described in detail elsewhere [19].  $\text{CaH}_2$  targets were sputtered with  $\text{Cs}^+$  ions, and negative ions were extracted from the ion source. The ion beam was mass-analyzed and particles of mass-to-charge ratio 44 ( $^{41}\text{CaH}_3^-$  ions) were injected into the accelerator. Electrons were removed from separated ions by gas stripping. Ions of charge state 4+ were selected to filter out molecular ions and to minimize parasitic  $\text{O}^{2+}$  and  $\text{S}^{4+}$  beams that render measurements of  $^{40}\text{Ca}$  ion beams difficult.

Measurements were performed at a terminal voltage of 5 MV. Typical ion currents of  $\text{CaH}_3^-$  were 400 nA for prepared samples and 800 nA for blanks and secondary standards made from commercially available  $\text{CaH}_2$ . Transmissions ranged from 10 to 16%. Particles were identified with a three-anode ionization chamber. A time-of-flight spectrometer was used to improve mass separation, in particular for efficient suppression of  $^{42}\text{CaH}_2^{4+}$  ions. Reported data are normalized to IRMM-3701.  $^{41}\text{Ca}/^{40}\text{Ca}$  ratios for chemical and instrumental blanks were  $1\text{--}2\times 10^{-13}$ . Average repeatability (1 SD) of independent isotope ratio measurements ( $n=5$ ) was 2.2%, with 90% of the data having a repeatability of <3.5%.

#### $^{41}\text{Ca}$ isotopic analysis by AMS (Lawrence Livermore National Laboratory)

Sample processing and measurement followed established procedures [18, 20, 21] with minor modifications. Chemicals were all of analytical grade, water was distilled and deionized, and all labware was single-use. CaO samples were dissolved in 1 ml 5 N  $\text{HNO}_3$  and brought up to 50 ml with water. Sample Ca solutions were loaded into resin beds previously prepared by rinsing sequentially with 10 ml of water, 5 N  $\text{HNO}_3$ , water and 0.08 N  $\text{HNO}_3$ , respectively. After sample loading, the resin beds were rinsed with 10 ml 0.08 N  $\text{HNO}_3$ . Sample Ca was eluted using 6 ml 5 N  $\text{HNO}_3$  and passed through the resin in three equal aliquots of 2 ml.

Solution pH was adjusted to produce a solution of ~0.5 M  $\text{H}^+$  through the addition of 1.5 ml of concentrated ammonium hydroxide, and after thorough mixing 2–3 ml of 48% HF was added. After at least 12 hours, the sample

CaF<sub>2</sub> was isolated via centrifugation, washed with 0.01 N HF, and dried overnight in a muffle furnace at 90 °C.

The CaF<sub>2</sub> prepared was mixed with silver powder (4 parts CaF<sub>2</sub> : 1 part Ag by mass) and pressed into aluminum AMS sample holders. Samples and concurrently produced standards and blanks were placed in the AMS ion source. <sup>41</sup>Ca/<sup>40</sup>Ca isotope ratios were measured in samples, standards and blanks as follows: (1) mass separation of CaF<sub>3</sub><sup>-</sup> molecules; (2) acceleration of these molecules through 9.1 million volts; (3) removal of nine electrons through charge exchange in a thin carbon foil at the high-voltage terminal; (4) a second acceleration to ground potential (final energy >76 MeV); (5) measurement of <sup>40</sup>Ca<sup>8+</sup> in an offset Faraday cup after mass analysis; (6) ion identification and single particle counting of <sup>41</sup>Ca<sup>8+</sup> in a multi-anode gas ionization detector after additional mass and velocity filters. Raw ratios of <sup>41</sup>Ca<sup>8+</sup> counts (collected for 100–200 s) to total <sup>40</sup>Ca<sup>8+</sup> charge (collected in 50 μs pulses at ~3 Hz) were calculated by the data collection system. Samples and standards were run at least four times, and final <sup>41</sup>Ca/Ca was calculated via normalization to the known standard ratios, and assuming natural <sup>40</sup>Ca abundance [22].

The unweighted average chemistry blank was <sup>41</sup>Ca/Ca = (1.5 ± 0.9) × 10<sup>-13</sup> for samples with <sup>41</sup>Ca/Ca < 10<sup>-8</sup>; above this level, minor ion source memory from high-<sup>41</sup>Ca samples produced a slightly higher background of (2.2 ± 0.5) × 10<sup>-12</sup>. The certified isotope reference materials IRMM-3701/4, /5, and /6 (Table 2) were each measured in triplicate, and AMS results were scattered around known values at a 1 SD reproducibility averaging 3–5% for the different standards. Because of an observed nonlinearity for IRMM-3701/3 (<sup>41</sup>Ca/<sup>40</sup>Ca = 10<sup>-8</sup>), the minimum uncertainty for samples with a <sup>41</sup>Ca/<sup>40</sup>Ca isotope ratio higher than 5 × 10<sup>-9</sup> was set to 10%.

**Table 2** Certified isotope amount ratios of the IRMM-3701 isotope reference materials used in this study to calibrate AMS and RIMS measurements against each other

Isotopic reference material	$n(^{41}\text{Ca})/n(^{40}\text{Ca})$
IRMM-3701/1	1.011 4(68) × 10 <sup>-6</sup>
IRMM-3701/2	1.023 5(69) × 10 <sup>-7</sup>
IRMM-3701/3	1.018 1(69) × 10 <sup>-8</sup>
IRMM-3701/4	1.047 9(71) × 10 <sup>-9</sup>
IRMM-3701/5	1.052 0(71) × 10 <sup>-10</sup>
IRMM-3701/6	1.091 3(74) × 10 <sup>-11</sup>
IRMM-3701/7	1.054 9(72) × 10 <sup>-12</sup>
IRMM-3701/8	1.052 4(71) × 10 <sup>-13</sup>

Uncertainties are given as expanded uncertainties ( $k=2$ ) and apply to the last two digits of the value.

#### <sup>41</sup>Ca isotopic analysis by RIMS (University of Mainz)

Ca separated from urine as CaO at the Laboratory of Human Nutrition, ETH Zurich, was dissolved in 1 ml 3M nitric acid and stored in solution. For analysis, about 10 μl of the Ca(NO<sub>3</sub>)<sub>2</sub> solution was brought onto a Ta carrier foil, dried at ~90 °C under normal pressure, and inserted into a graphite furnace. The oven was introduced into a small high-vacuum chamber via a fast vacuum lock and Ca was reduced and atomized to form an atomic beam at temperatures of around 1600 °C. Selective ionization was carried out by resonant optical excitation using a system of three commercial continuous diode lasers (Model DL100, TUI Optics GmbH, Gräfeling, Germany). For the first excitation step, red diode laser light was converted into the blue spectral region by a custom-designed frequency doubling unit. Selectively excited Ca atoms were ionized by a CO<sub>2</sub> laser (48-2W, EXCEL Technology Europe GmbH, Fürstfeldbruck, Germany) and mass-analyzed using a quadrupole mass spectrometer (QMS, MEXM64, ABB Extrel, Pittsburgh, PA, USA). The exact amount of transferred isotopic label was determined by reweighing the glass vials. Quantitative low-background ion detection was carried out by a channeltron (402A-H, De Tech, Palmer, MA, USA).

To determine the Ca isotope ratios, the laser and QMS were tuned alternately to different resonance positions and count rates were taken. Specifications for an overall efficiency of >10<sup>-5</sup>, with a relative limit of detection of 2 × 10<sup>-13</sup> for the <sup>41</sup>Ca/<sup>40</sup>Ca ratio, and with a repeatability of about 5%, had been demonstrated previously [23].

#### <sup>41</sup>Ca reference material

To calibrate the different mass spectrometric techniques against each other, a series of isotopic reference materials for <sup>41</sup>Ca (IRMM-3701) was produced and certified for isotope amount ratios [15]. The IRMM-3701 series covers a range of <sup>41</sup>Ca/<sup>40</sup>Ca isotope amount ratios from 10<sup>-6</sup> to 10<sup>-13</sup> (Table 2). It is derived from the gravimetric mixing of a <sup>41</sup>Ca solution (IM-6010), which was certified for Ca amount content and isotopic composition, and a Ca solution prepared from CaCO<sub>3</sub> (99.95% purity, Merck, Darmstadt, Germany) of natural isotopic composition. The <sup>41</sup>Ca/<sup>40</sup>Ca isotope amount ratio of the CaCO<sub>3</sub>, as measured by AMS, was below the limit of detection (5 × 10<sup>-14</sup>). The <sup>41</sup>Ca/<sup>40</sup>Ca isotope amount ratios of the series have been measured independently by AMS and RIMS over the total range. Linearity was excellent for both techniques [15]. The RIMS measurements presented were normalized to IRMM-3701 to ensure the comparability of the <sup>41</sup>Ca data generated. For the AMS measurements, concurrent check standards were prepared. The AMS data matched the IRMM-3701 standards within the measurement uncertainty.

## Total calcium analysis

Total Ca was determined directly in urine samples at the Laboratory of Human Nutrition, ETH Zurich, by flame atomic absorption spectrometry (SpectrAA 400, Mulgrave, Australia) in an air/acetylene flame after appropriate dilution (1:20 to 1:50) with an acidified 0.5% (w/v) lanthanum chloride solution. A commercial aqueous standard (Titrisol, Merck, Darmstadt, Germany) was used for internal standard addition. Quality control material was processed in parallel with urine (Lyphocheck, Quantitative Urine Control, BioRad, Anaheim, CA, USA). Ca analysis of the test meal was performed using the standard addition technique after microwave digestion using a  $\text{HNO}_3/\text{H}_2\text{O}_2$  mixture. The average repeatability was 3.5% RSD for independent runs of the same samples.

## Urinary $^{41}\text{Ca}$ excretion pattern

**Combined power/exponential law analysis** The retention systematics of bone-seeking elements such as Ca were investigated earlier using radioisotopic techniques and described by a combined power/exponential law [13, 24]. This analysis arose in the 1960s and early 1970s, when researchers had limited computer access and thus sought “simpler and computationally more tractable models [that] can be formulated using other mathematical functions, such as power functions” [25]. As the urinary excretion of an administered Ca tracer over time is a derivative of retention, it can be described by

$$E(t) = A \cdot t^B + C \cdot e^{Dt} \quad (1)$$

where  $E(t)$  is the Ca amount or concentration in urine and  $A$ ,  $B$ ,  $C$  and  $D$  are parameters reflecting individual differences in urinary tracer excretion. The individual parameters  $A$ ,  $B$ ,  $C$  and  $D$  were determined for each subject by fitting the curve described by Eq. 1 to observed  $^{41}\text{Ca}$  data in urine. Data were analyzed using commercial software (Origin 7, OriginLab Corporation, Northampton, MA, USA). Analytical errors ( $\sigma$ ) in the individual data points were taken into account by weighting data points for measurement precision ( $w=1/\sigma^2$ ).

**Population pharmacokinetic analysis** In parallel with the combined power/exponential fitting procedures described above, data were also fitted to several compartmental models using population pharmacokinetics. If compartmental models are used, it can be assumed that a drug or any other compound, such as an isotopic tracer administered to the human body, distributes and exchanges between a series of compartments [26]. These compartments may, but do not have to, represent anatomic spaces such as organs or body tissues. The concentrations of the tracer in plasma, urine and/or feces over the time of the study will thus depend on

the transfer rates between compartments and the compartment volumes. Accordingly, transfer rates and compartment volumes represent the parameters  $P_i$  to be estimated based on the observed concentration data  $y_{ij}$ , i.e.:

$$y_{ij} = f(t_{ij}, P_i) \cdot e^{\varepsilon_{1ij}} + \varepsilon_{2ij} \quad (2)$$

where  $f$  represents the function describing the compartmental model, evaluated at time  $t_{ij}$  for subject  $i$  studied at time  $j$ , whereas  $\varepsilon_{1ij}$  and  $\varepsilon_{2ij}$  represent the heteroscedastic and homoscedastic residual variabilities, which cover analytical error, within-subject variability and model misspecification. In population pharmacokinetics, the parameters of subject  $i$ ,  $P_i$ , are in turn expressed as

$$P_i = g(\theta, Z_i) + \eta_i \quad (3)$$

where  $g$  is a function of  $\theta$ , a vector of unknown parameters assumed to have the same value in each subject (the fixed effects),  $Z$  is the subject's characteristics (e.g., age, body weight), and  $\eta$  is a vector of unknown parameters belonging to subject  $i$  (the random effects). The parameter  $\eta$  is assumed to be multivariate and normally distributed with a mean of 0 and with variances to be estimated [27–29]. To do so, the data on urinary  $^{41}\text{Ca}$  excretion from the 22 study participants were combined into one data set, and fit jointly to the different compartmental models using the first-order method (FO) of the commercial Nonlinear Mixed Effects Modeling Method Software (NONMEM, version V, running with NM-TRAN version II, University of California, San Francisco, CA, USA). The statistical model accounting for intra-individual variability consisted of an exponential error and an additive error term (see Eq. 2). We thus used maximum likelihood (ML) for curve fitting and mixed-effects regression (fixed and random) to estimate population means and variances of kinetic parameters (NONMEM Users Guides, University of California, San Francisco, CA, USA). Furthermore, the POSTHOC option was applied to obtain individual parameter estimates and individual concentration predictions after the analysis.

A stepwise procedure was used to identify the model that describes the experimental data best. There are three different criteria used to compare the different models: the Schwarz information criterion ( $BIC$ ), the Akaike criterion ( $AIC$ ) or the Hannan–Quinn criterion ( $HQ$ ). It has been shown, however, that the  $BIC$  is the most conservative criterion of these three [30], and it was therefore selected as the most appropriate tool to avoid overfitting of the data. The  $BIC$  depends on the objective function  $OF$ , the overall number  $p$  of (fixed and random effect) parameters to be estimated, and the number of data points  $N$  in the dataset.

$$BIC = OF + p \cdot \log(N) \quad (4)$$

where the  $OF$  corresponds to minus twice the logarithm of the likelihood, and can be directly obtained from the NONMEM output [31]. Thus, the  $BIC$  favors models which describe the data appropriately, i.e., that exhibit the lowest  $OF$ , and also take into account the number of parameters in order to avoid overfitting of the data. For models with rather small  $BIC$  differences, we compared interindividual variability estimates, intraindividual variability estimates, normalized root mean square errors (NRMSE) and normalized mean error (NME) of the differences between measurements and predictions.

The  $^{41}\text{Ca}/^{40}\text{Ca}$  isotope ratio was chosen for data evaluation. Because of the high natural abundance of  $^{40}\text{Ca}$  of 96.941% [32], it can be regarded as a proxy for the  $^{41}\text{Ca}/\text{Ca}$  ratio. To calculate the kinetic parameters, the initial dose of  $^{41}\text{Ca}$  entering compartment 1 and the concentration of  $^{41}\text{Ca}$  in this compartment over the 700-day monitoring period were required. As these variables could not be directly measured in the study, they had to be set to reasonable a priori guesses. As the  $^{41}\text{Ca}$  dose was administered orally, an assumption for the bioavailability had to be made in order to assess the amount of tracer transferred from the intestine into compartment 1 to estimate an “iv proxy dose.” An absorption efficiency of 50% was assumed, as we observed from a recent study on the same subjects that Ca absorption from a similar standardized test meal was  $51.2 \pm 8.9\%$  (Denk E, Walczyk T, Hurrell RF, manuscript in preparation). At an oral  $^{41}\text{Ca}$  dose of  $2.35 \times 10^{-5}$  mmol, this results into an “iv proxy dose” of  $1.18 \times 10^{-5}$  mmol. It is not expected that variations in Ca absorption efficiency have any influence on the outcome of the model-finding procedure, since any possible difference between the assumed and actual dose of the tracer reaching the systemic circulation would just shift the urinary  $^{41}\text{Ca}$  excretion pattern up or down. The shape of the curve, which determines the kinetic model, would not be changed. Such a difference would induce at most a change in the pool size of compartment one ( $V_1$ ) and thus any derived absolute transfer rates in mg Ca per day, respectively. For this reason, transfer rates are given in relative and not in absolute terms.

In order to assess changes in the  $^{41}\text{Ca}$  concentration in compartment 1 over time, the urinary  $^{41}\text{Ca}/^{40}\text{Ca}$  isotope ratios had to be transformed into  $^{41}\text{Ca}$  concentrations in plasma. Physiologically, compartment 1 probably corresponds to Ca in extracellular fluids (ECF) and the cellular pool. In the ECF and in the cellular compartment, the concentration of ionized Ca is maintained within the narrow range of 1.15–1.25 mmol/l [33]. As discussed before, urinary  $^{41}\text{Ca}/^{40}\text{Ca}$  isotope ratios can be regarded as substitutes for the  $^{41}\text{Ca}/^{40}\text{Ca}$  isotope ratios in plasma. Therefore, urinary  $^{41}\text{Ca}/^{40}\text{Ca}$  isotope ratios could be transformed into  $^{41}\text{Ca}$  concentrations in plasma based on a mean concentration for plasma Ca of 1.2 mmol/l. Based on the calculated  $^{41}\text{Ca}$  “iv proxy dose” and the  $^{41}\text{Ca}$  concentration in compartment 1, the kinetic parameters of the final model were obtained.

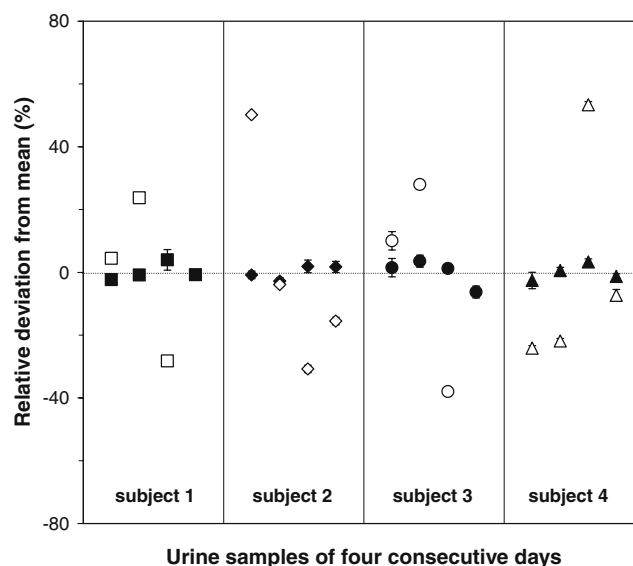
## Results and discussion

### Subject characteristics

Three out of the 25 subjects did not complete the study. One subject had to be excluded from the study due to illness. Another subject experienced a fracture. A third subject died of other causes during the study. Data from the three subjects were excluded from all analyses. The remaining 22 subjects were  $66.7 \pm 4.9$  years at the beginning of the study and had a mean body mass index of  $26.1 \pm 3.3$  kg/m<sup>2</sup>. Mean Ca intake assessed by food frequency questionnaire was  $803 \pm 257$  mg Ca per day and BMD was  $-1.48 \pm 0.72$  (T-score in femur neck) at the beginning of the study.

### Assessment of urinary $^{41}\text{Ca}$ excretion

In order to assess the biological variability of the  $^{41}\text{Ca}$  signal, 24-h urine samples of four subjects of subgroup B were collected on four consecutive days after a labeling period of 240 days. Significant variations in the daily amount of excreted  $^{41}\text{Ca}$  were observed in each individual (RSD: 26.3–36.3%), as derived from the urinary  $^{41}\text{Ca}/^{40}\text{Ca}$  isotope ratio and the Ca amount excreted in urine. As expected, daily urinary Ca losses showed significant intra-individual variations (RSD: 28.3–36.2%). Intra-individual variations, however, were much smaller for the urinary  $^{41}\text{Ca}/^{40}\text{Ca}$  isotope ratio (RSD: 2.2–4.3%), see Fig. 2.



**Fig. 2** Variations in the urinary  $^{41}\text{Ca}/^{40}\text{Ca}$  isotope ratio (full symbols) and the total amount of  $^{41}\text{Ca}$  (open symbols) on four consecutive days, as observed in the 24-h urine samples collected. Data are plotted as the relative deviation from the mean over all four urine samples from the same subject



Although urinary Ca losses varied strongly between days, this did not affect the urinary  $^{41}\text{Ca}/^{40}\text{Ca}$  isotope ratio significantly. This is in agreement with basic principles of human Ca metabolism. Ca in plasma is effectively reabsorbed in the kidneys and only a small fraction passing through the kidneys (<1%) is inevitably lost in urine. This fraction can vary significantly in the individual within and between days, depending on diet and lifestyle factors [34]. Because the human body cannot distinguish between Ca isotopes within the measurement errors of the applied techniques, it can be assumed that equal fractions of natural Ca and  $^{41}\text{Ca}$  are transferred from plasma into urine. The urinary  $^{41}\text{Ca}/^{40}\text{Ca}$  isotope ratio thus becomes a direct measure of the isotopic composition of plasma Ca, which is more stable than the  $^{41}\text{Ca}$  amount excreted in urine. This has been confirmed recently [21], and makes the urinary  $^{41}\text{Ca}/^{40}\text{Ca}$  isotope ratio the measure of choice for monitoring changes in bone Ca metabolism. Because Ca concentration in plasma is subject to close homeostasis within a narrow range, and plasma volume likewise shows only small variations, the amount of circulating natural Ca in plasma is highly constant in the individual. Thus, changes in the urinary  $^{41}\text{Ca}/^{40}\text{Ca}$  isotope ratio directly reflect changes in  $^{41}\text{Ca}$  concentration as well as changes in the circulating  $^{41}\text{Ca}$  amount in plasma.

## Kinetics of urinary $^{41}\text{Ca}$ excretion

### Combined power/exponential analysis

In the era before readily available computing power, the systematics of urinary  $^{41}\text{Ca}$  excretion were described by a function consisting of an exponential term and a power term (see Eq. 1). For subjects from subgroups A, B and C, enough data points were available to fit parameters in Eq. 1 to the observed data points. For subjects in subgroup D, analysis was limited to 2–3 samples per individual, which is not sufficient to solve Eq. 1. According to [13], the exponential term of the function becomes negligible at intervals greater than 30 days after dose administration, and so labeling curves can be described by the power term alone after that:

$$E(t) = A \cdot t^B \quad (5)$$

By using Eq. 5, labeling curves were established for three subjects (subgroup D) using the three data points obtained within the later part of the labeling phase (>150 days). Calculated parameters describing the changes in the urinary  $^{41}\text{Ca}/^{40}\text{Ca}$  isotope ratio according to Eqs. 1 and 5 are given in Table 3. The data obtained for tracer excretion from all subjects are plotted in Fig. 4. From the data presented in Table 3, it is apparent that urinary tracer excretion can be

**Table 3** Parameters describing changes in urinary  $^{41}\text{Ca}/^{40}\text{Ca}$  isotope ratios with time based on a combined power/exponential law ( $E(t) = At^B + Ce^{Dt}$ )

Subgroup	Subject ID	No. of measurements	$R^2$	$A$	$B$	$C$	$D$
A	1	31	0.969	$27.10(76) \times 10^{-9}$	-0.8249(52)	$49.11(42) \times 10^{-9}$	-0.09253(45)
	2	28	0.982	$22.40(83) \times 10^{-9}$	-0.7732(63)	$58.64(48) \times 10^{-9}$	-0.09054(47)
	3	25	0.971	$11.80(49) \times 10^{-9}$	-0.6117(70)	$51.75(85) \times 10^{-9}$	-0.07664(62)
	4	30	0.968	$8.93(22) \times 10^{-9}$	-0.6380(46)	$57.84(54) \times 10^{-9}$	-0.119917(57)
	5	21	0.989	$9.62(32) \times 10^{-9}$	-0.6316(57)	$55.77(57) \times 10^{-9}$	-0.10937(74)
	6	23	0.926	$9.21(31) \times 10^{-9}$	-0.5501(58)	$63.92(60) \times 10^{-9}$	-0.098772(59)
B	7	11	0.969	$4.3(2.5) \times 10^{-11}$	0.248(99)	$2.51(21) \times 10^{-8}$	-0.0640(40)
	8	13	0.932	$2.9(3.2) \times 10^{-9}$	-0.46(19)	$5.88(53) \times 10^{-8}$	-0.0720(40)
	9	15	0.971	$5.6(1.7) \times 10^{-8}$	-0.900(51)	$0.47(12) \times 10^{-7}$	-0.119(18)
	10	12	0.9	$4.3(1.2) \times 10^{-9}$	-0.476(46)	$2.65(47) \times 10^{-8}$	-0.0740(70)
C	11	8	0.999	$68.93(79) \times 10^{-8}$	-1.4550(26)	$24.49(15) \times 10^{-9}$	-0.1086(54)
	12	8	0.999	$121.63(68) \times 10^{-9}$	-1.0359(10)	$86.51(35) \times 10^{-9}$	-0.123770(20)
	13	7	0.999	$7.96(11) \times 10^{-8}$	-1.0903(30)	$653.53(63) \times 10^{-10}$	-0.10410(10)
	14	7	0.999	$14.70(11) \times 10^{-8}$	-1.0716(17)	$454.06(65) \times 10^{-10}$	-0.10435(15)
	15	7	0.999	$13.60(11) \times 10^{-8}$	-1.0850(18)	$486.23(98) \times 10^{-10}$	-0.09430(30)
	16	11	0.989	$6.92(43) \times 10^{-9}$	-0.550(12)	$0.36(12) \times 10^{-7}$	-0.0715(88)
	17	7	0.999	$84.40(33) \times 10^{-8}$	-1.4174(10)	$1.1(7.9) \times 10^{-3}$	-0.62(33)
	18	7	0.999	$25.10(26) \times 10^{-8}$	-1.1520(20)	$50.70(11) \times 10^{-9}$	-0.10095(30)
	19	7	0.996	$10.50(33) \times 10^{-11}$	0.2898(61)	$3811.14(62) \times 10^{-11}$	-0.048120(10)
D	20	2	1	$88(-) \times 10^{-11}$	-0.225(-)	-	-
	21	3	0.895	$3.78(14) \times 10^{-9}$	-0.3930(70)	-	-
	22	3	0.804	$6.73(72) \times 10^{-9}$	-0.562(20)	-	-

Parameters A–D were obtained for each individual subject by fitting the curve to the experimental data. For subjects 14–16, only power term parameters were assessed based on data points obtained >150 days after isotope administration (see text). Uncertainties in the two last significant digits (1 SD) are given in parentheses.

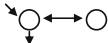
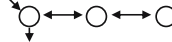

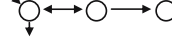

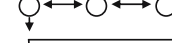

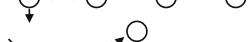



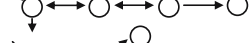
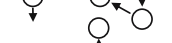

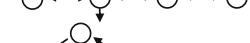
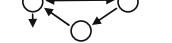

better described for subgroups A, B and C ( $R^2=0.90-0.99$ ) than for subgroup D ( $R^2=0.80-1.00$ ) using nonlinear curve-fitting techniques. This can be attributed to either the limited number of data points available and/or the use of Eq. 5 to describe tracer kinetics for subgroup D, which does not consider the early phase of tracer excretion (<100 days post-dose).

#### Selection of the appropriate compartmental model using population pharmacokinetics

The pharmacokinetic data collected in these 22 subjects for up to 700 days permit the evaluation and comparison of

several compartmental models for describing Ca distribution within, and elimination from, the human body. Ca distribution and excretion is described as a series of compartments representing Ca pools that exchange with defined Ca transfer rates  $k$ . This analysis considers the urinary  $^{41}\text{Ca}/^{40}\text{Ca}$  isotope ratio to be a monitor of the  $^{41}\text{Ca}/^{40}\text{Ca}$  isotope ratio in plasma. The process used to find a suitable model started with the use of a basic compartmental model consisting of two compartments (Table 4, model 1). The inclusion of a third compartment resulted in a decrease in the  $BIC$  of at least 255 units, indicating a considerable improvement of the fit of the  $^{41}\text{Ca}/^{40}\text{Ca}$  isotope ratio data (Table 4, models 2–6).

**Table 4** Identification of the model that describes experimental data for urinary  $^{41}\text{Ca}$  excretion best

Compartment model	$p$ (fixed+random)	OF	BIC
(1) 	8 (4+4)	622.8	642.3
(2) 	12 (6+6)	355.2	384.5
(3) 	12 (6+6)	355.5	384.8
(4) 	12 (6+6)	358.0	387.3
(5) 	12 (6+6)	358.0	387.3
(6) 	12 (6+6)	355.2	386.9
(7) 	16 (8+8)	355.2	394.3
(8) 	16 (8+8)	355.1	394.2
(9) 	16 (8+8)	349.3	388.4
(10) 	16 (8+8)	349.0	388.1
(11) 	16 (8+8)	348.3	387.4
(12) 	16 (8+8)	347.8	386.9
(13) 	16 (8+8)	347.8	386.9
(14) 	16 (8+8)	347.2	386.3
(15) 	16 (8+8)	342.7	381.8
(16) 	16 (8+8)	341.6	380.7
(17) 	20 (10+10)	347.5	396.4

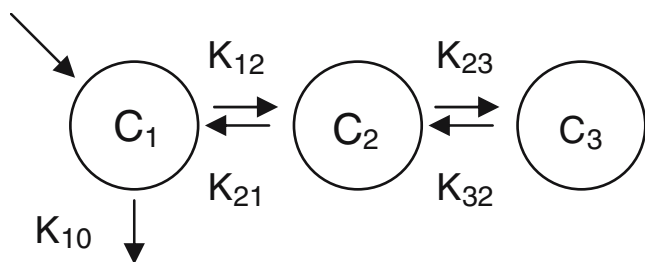
Model finding was performed by NONMEM population pharmacokinetic analysis using all data obtained for the 22 subjects in the study. The BIC-criterion is calculated as the sum of the NONMEM objective function (OF) and number of estimated parameters ( $p$ ) in the model multiplied with the log of the number of observations in the study ( $N=278$ ) (Eq. 3). Model 2 was found to best describe observations based on the minimum BIC value. For models 15 and 16, a slight reduction of the BIC value by 2.7 to 3.8 units compared with model 2 was observed. However, residual plots for models 15 or 16 did not show any improvement. NRMSE and NME for the differences between observations and predictions were higher for model 15 (NRMSE: 0.297, NME: 0.021) and model 16 (NRMSE: 0.386, NME: 0.168) when compared with model 2 (NRMSE: 0.285, NME 0.016).

Since models 2 and 3 exhibited a lower *BIC* than the other three-compartment models tested (Table 4, models 4–6), we selected these two models for further evaluation. Both models exhibit comparable *BIC* values (384.5 and 384.8), indicating equally good descriptions of the data. Furthermore, the residual plots and the variability estimates were comparable between both models, with model 2 a sequential model and model 3 a Y-type model. Many recent models [35–37] use a series model, although various authors [25, 38] have pointed out the equivalence of the various branching schemes, concluding that the choice of model architecture is ultimately heuristic.

In addition, we tested several four-compartment models which appeared to be physiologically meaningful (Table 4, models 7–16). However, most of these models did not reduce the *BIC* any further when compared with the proposed three-compartment model 2. Slight reductions in the *BIC* by 2.7 to 3.8 units were observed for models 15 and 16. However, no visual improvement of the fits could be detected. Furthermore, the residual plots did not show any improvement from model 2 to model 15 or 16. This small difference was confirmed by slight increases in NRMSE and NME for the differences between observations and predictions for model 15 (NRMSE: 0.297, NME: 0.021) and model 16 (NRMSE: 0.386, NME: 0.168) in comparison with model 2 (NRMSE: 0.285, NME: 0.016). We thus concluded that none of the four-compartment models described the population data better than the proposed three-compartment model 2 in Table 4. Furthermore, a five-compartment model (Table 4, model 18) was tested which also did not improve the *BIC*. We thus concluded that the sequential three-compartment model 2 in Table 4 best describes the data over the time periods represented.

#### Description of the model

The final model, given schematically in Fig. 3, is defined by the following series of equations defining the transfer



**Fig. 3** Compartmental model that was found to best describe the observed  $^{41}\text{Ca}$  tracer kinetics. Compartments can, but do not have to, correspond directly to anatomic spaces. The  $^{41}\text{Ca}$  tracer enters the central compartment, to which the dose was administered (compartment  $C_1$ ), and is transferred to a fast exchanging pool (compartment  $C_2$ ), from where it is transferred to a slowly exchanging Ca pool in the body (compartment  $C_3$ ), probably located in bone

rates ( $k_{12}$ ,  $k_{21}$ ,  $k_{23}$ ,  $k_{32}$ ) between the three compartments, the elimination rate ( $k_{10}$ ) from compartment 1 and the volume of compartment 1 ( $V_1$ ) using a series of fixed ( $\theta_{1-6}$ ) and random ( $\eta_{1-4}$ ) effect parameters:

$$k_{12} = \theta_1 \cdot e^{\eta_1} \quad (6)$$

$$k_{21} = \theta_2 \cdot e^{\eta_2} \quad (7)$$

$$k_{23} = \theta_3 \cdot e^{\eta_3} \quad (8)$$

$$k_{32} = \theta_4 \cdot e^{\eta_4} \quad (9)$$

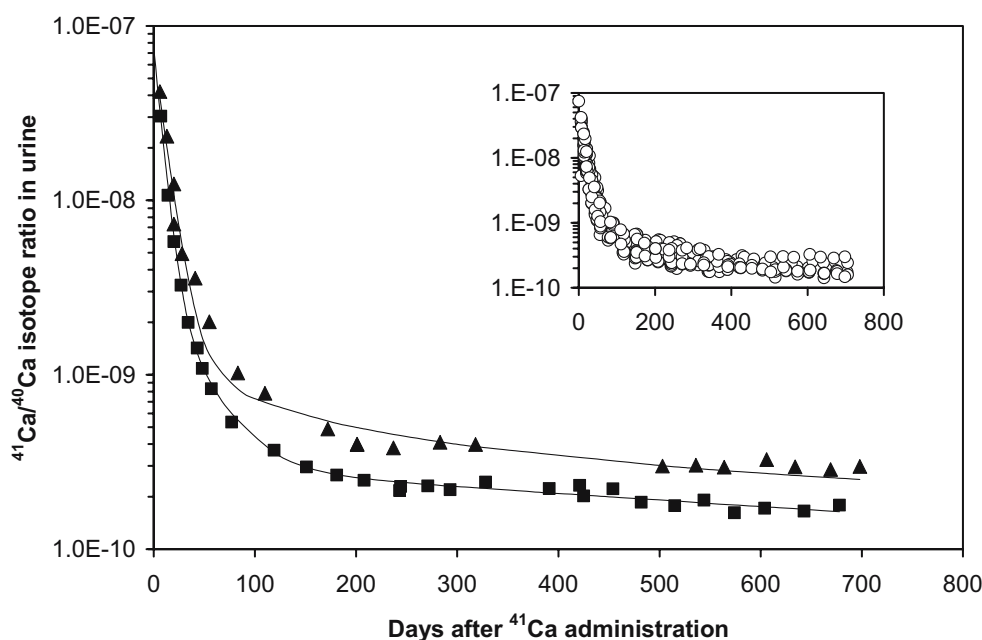
$$k_{10} = \theta_5 \cdot e^{\eta_5} \quad (10)$$

$$V_1 = \theta_6 \cdot e^{\eta_6} \quad (11)$$

The fixed effect parameters are common to all individuals, whereas each individual has its own random effect parameters. Since each of the random effect parameters exhibit a mean of 0, the  $\theta$  values represent the mean parameters of the population, whereas their variability is estimated as being the variances of the random effect parameters  $\eta$ . The initial statistical model included an exponential error and an additive error term accounting for intra-individual variability. It was found that the additive error term became negligible during analysis and it was therefore excluded (data not shown). Figure 4 gives the population prediction and the data for all individuals, and Table 5 lists all parameter estimates.

It is important to reiterate that the compartments may not correspond directly to anatomic spaces but best describe the  $^{41}\text{Ca}$  tracer kinetics: the tracer enters the central (i.e., the dosing) compartment (compartment 1), it is transferred to a fast exchanging pool (compartment 2), from where it is transferred to a slowly exchanging Ca pool within the body (compartment 3), probably predominantly located in bone (see Fig. 3). Transfer rates obtained for this model refer to long-term  $^{41}\text{Ca}$  tracer kinetics. Conventional techniques used to determine tracee (i.e., natural Ca) kinetics from tracer data are usually performed over 1–2 weeks. This requires the assumption of a steady state (zero net Ca balance) for body Ca, which can hold for short-term studies, but may not hold for our experiment in which postmenopausal women were followed up to two years post-dosing.

**Fig. 4** Kinetics of urinary  $^{41}\text{Ca}$  excretion in all subjects (*open circles*). Datasets of two representative subjects (ID 20, *squares*, and 22, *triangles*) were described by curves obtained from the computed population prediction (NONMEM) for the sequential three-compartmental model illustrated in Fig. 3. The  $^{41}\text{Ca}$  urinary excretion data for all subjects are shown in the *inset*



#### *Combined power law/exponential versus pharmacokinetic compartmental analysis*

For direct comparison purposes, the relative deviations between predicted and measured values for the power/exponential analysis and the compartmental model are presented in Fig. 5 as relative differences in percent for the six subjects of subgroup A at each sampling time point during the 700-day labeling period. Mean deviations of measurements from predictions for the noncompartmental approach were  $(-10 \pm 7)\%$  for negative and  $(15 \pm 12)\%$  for positive divergence, totaling  $(-1 \pm 13)\%$ . For the compartmental modeling approach, relative differences between modeled data and  $^{41}\text{Ca}$  measurements were  $(-6 \pm 5)\%$  for negative and  $(-6 \pm 4)\%$  for positive divergence at a combined divergence of  $(0 \pm 7)\%$ . This clearly demonstrates the advantages of the compartmental analysis approach. For this technique, relative differences between measured and modeled data points were found to be smaller and more balanced between negative and positive divergence, indicating a better description of the data than obtained by the modeled curve. Fits based on the use of a combined exponential/power law to describe urinary tracer excretion showed substantially higher deviations, which were fairly unbalanced between negative and positive divergence. Positive and negative divergences between measured and predicted data points for compartmental analysis were symmetric during the 700-day labeling period, and significantly smaller. Long-term variability of divergence (1 SD) was 4% from day 150 after isotope administration, which is higher than the short-term variability of the  $^{41}\text{Ca}$  signal ( $\sim 3\%$ ), determined over five days. This translates into a detection limit for a shift in the  $^{41}\text{Ca}$  signal of 12% when a

single urine sample is analyzed at the end of the intervention period.

Use of  $^{41}\text{Ca}$  as a tool to assess the impact of interventions on bone health

#### *Start of a possible intervention*

$^{41}\text{Ca}$  may provide a powerful tool for directly monitoring changes in bone metabolism in response to an intervention to a sensitivity that is expected to surpass the power of conventional techniques. For these applications, however, meaningful information can only be obtained when urinary  $^{41}\text{Ca}$  originates mainly from bone. To identify this stage within the labeling process, changes in  $^{41}\text{Ca}$  distribution between the compartments with time were calculated using the population parameters in Eqs. 5–11 (see Fig. 6). Following administration, the tracer is quickly transferred from the central compartment ( $C_1$ ) to the fast exchanging compartment ( $C_2$ ). A maximum amount of the tracer in  $C_2$  can be found 20–30 days post-dosing. After that,  $^{41}\text{Ca}$  is successively transferred from the fast exchanging compartment to the slowly exchanging bone compartment ( $C_3$ ) (see Fig. 3). The maximum amount of the  $^{41}\text{Ca}$  in this compartment is reached after 150–250 days. While changes in bone formation and resorption can be identified, in principle, by monitoring urinary  $^{41}\text{Ca}$  excretion over the first few weeks post-dosing, a more reliable assessment of the effect of intervention is possible after  $\sim 150$  days post-dosing, when excreted tracer mainly originates from bone.

We propose that an intervention can be started after the amount of  $^{41}\text{Ca}$  in compartment 3 (see Fig. 6) has reached a maximum, i.e., at least 150 days after  $^{41}\text{Ca}$  administration,

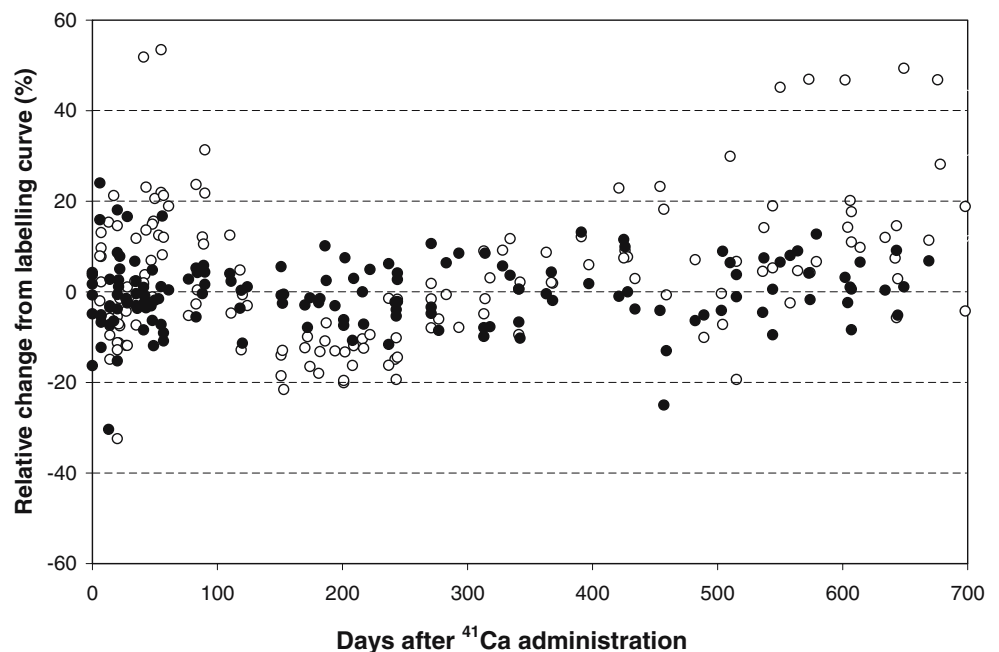
**Table 5** Parameters describing the changes in urinary  $^{41}\text{Ca}/^{40}\text{Ca}$  isotope ratios with time, obtained based on a sequential three-compartment model as illustrated in Fig. 3

	ID	$K_{10}$	$K_{12}$	$K_{21}$	$K_{23}$	$K_{32}$	$V_1$
Population parameters	Estimate	0.065	0.041	0.015	0.020	0.0041	65.5
	SE (%)	19.7	8.6	50.6	8.3	20.0	14.7
Inter-individual variability (*)	% Estimate	0.018	0.058	0.105	0.014	0.0503	0.01
	SE (%)	0.1	0.1	0.8	0.2	0.3	0.1
Individual parameters	1	0.065	0.050	0.012	0.019	0.0033	67.1
	2	0.071	0.037	0.017	0.019	0.0048	64.8
	3	0.059	0.041	0.014	0.019	0.0046	66.0
	4	0.076	0.059	0.010	0.021	0.0045	69.3
	5	0.075	0.049	0.012	0.020	0.0051	70.5
	6	0.057	0.060	0.013	0.021	0.0036	60.2
	7	0.078	0.047	0.012	0.020	0.0039	72.5
	8	0.067	0.029	0.021	0.022	0.0047	66.6
	9	0.076	0.054	0.015	0.018	0.0039	57.1
	10	0.071	0.054	0.011	0.022	0.0049	68.2
	11	0.064	0.041	0.017	0.019	0.0037	65.5
	12	0.056	0.052	0.012	0.020	0.0053	61.0
	13	0.071	0.035	0.012	0.020	0.0039	65.0
	14	0.060	0.050	0.016	0.019	0.0051	63.0
	15	0.062	0.040	0.015	0.019	0.0044	63.7
	16	0.066	0.042	0.014	0.021	0.0048	66.2
	17	0.058	0.039	0.019	0.019	0.0039	62.3
	18	0.056	0.042	0.017	0.019	0.0048	60.8
	19	0.055	0.034	0.028	0.018	0.0034	70.0
	20	0.071	0.039	0.014	0.021	0.0039	67.3
	21	0.061	0.046	0.016	0.020	0.0049	63.2
	22	0.066	0.042	0.015	0.020	0.0042	65.7

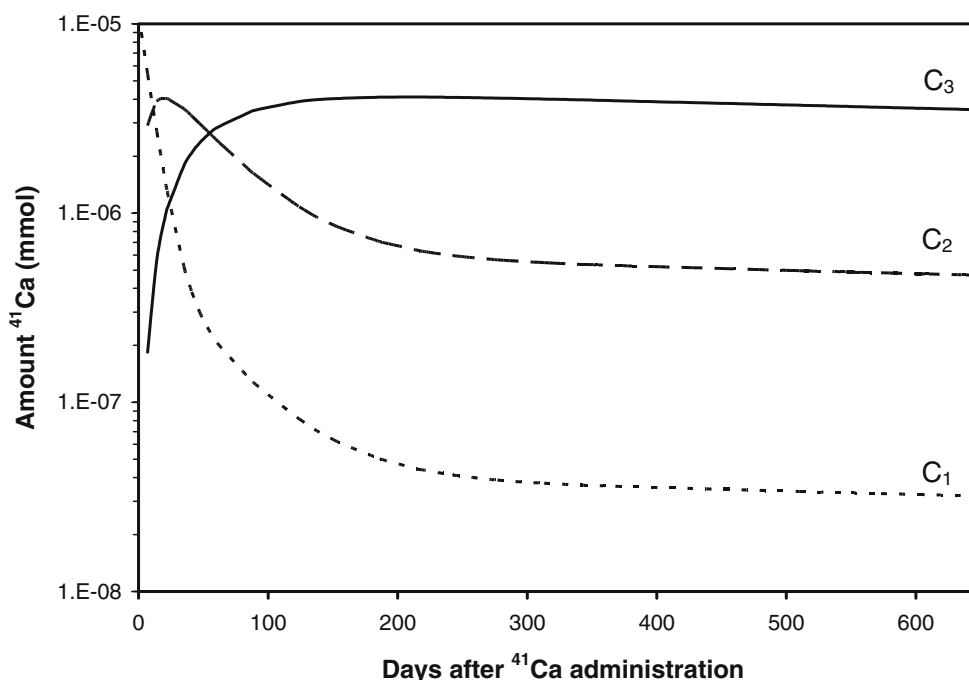
(\*) Intra-individual variability:  $9.6 \pm 4.5$  [% estimate  $\pm$  SE (%)]

Individual parameters (mean  $\pm$  SE) and population parameters, including inter-individual and intra-individual variability, are given for each transfer rate  $k_{ij}$  in fractions per day and for the volume term  $V_1$  in liters.

**Fig. 5** Relative differences (%) between measured and calculated  $^{41}\text{Ca}/^{40}\text{Ca}$  isotope ratios, as obtained by applying a combined exponential/power law (open circles) or population prediction (NONMEM) of the sequential three-compartmental model (filled circles) to describe the run of the curve for urinary  $^{41}\text{Ca}$  excretion. Data are presented for the six subjects of subgroup A, in which urinary  $^{41}\text{Ca}$  excretion was monitored up to 700 days after a single oral dose of  $^{41}\text{Ca}$  (day 0)



**Fig. 6** Calculated changes in  $^{41}\text{Ca}$  distribution with time between the three compartments ( $C_1$ ,  $C_2$ ,  $C_3$ ) (see Fig. 3), as identified by population prediction (NONMEM) of the sequential three-compartmental model for the data from all subjects



when the internal pools have reached stable equilibrium and the excreta constitute a steady but small loss. After this, the tracer signal would be expected to reflect bone resorption and accretion processes. Due to the activity of osteoclasts (cells specialized for bone resorption),  $^{41}\text{Ca}$  is successively resorbed from the bone matrix and transferred to plasma. It is partly excreted in urine and partly reincorporated into bone matrix by remineralization in the bone accretion process. Both processes determine the changes in the amount of  $^{41}\text{Ca}$  circulating in plasma, which can be monitored via the  $^{41}\text{Ca}/^{40}\text{Ca}$  isotope ratio in urine.

#### *Identifying the effect of intervention on bone health using $^{41}\text{Ca}$*

To evaluate the effect of intervention on bone resorption and accretion, the specific excretion pattern of the tracer may serve as a fixed index from which changes are measured. An intervention which affects bone resorption or formation will induce a shift in the urinary  $^{41}\text{Ca}/^{40}\text{Ca}$  isotope ratio (see Fig. 1).

The effect of a possible intervention can be evaluated by calculating the relative difference between the actual urinary  $^{41}\text{Ca}/^{40}\text{Ca}$  isotope ratios during an intervention and their values derived from the extrapolated run of the labeling curve as the reference. This requires a proper mathematical description of the labeling curve that allows for extrapolation to any time point during the intervention. In order to evaluate how well urinary  $^{41}\text{Ca}/^{40}\text{Ca}$  isotope ratios obtained for the labeling phase can be extrapolated to later time points, labeling curves were computed for assumed labeling periods of 200, 300, 400 and 500 days,

respectively, based on measured  $^{41}\text{Ca}$  data for the subjects in subgroup A. For these subjects, data points from up to 700 days after dose administration were available, which could be used to model a maximum labeling interval of 500 days and a maximum duration of the subsequent intervention period of 180 days. To assess the predictive power of the different labeling intervals, computed labeling curves for the different labeling periods were extrapolated to day 90 and day 180 of an assumed intervention and compared with the actual measurements at the same time points. For the evaluation, relative differences between measured and calculated data points at day 90 and day 180 of the intervention were assessed in each individual subject for the different labeling periods (200, 300, 400 and 500 days, respectively), see Table 6. Results indicate that the accuracy of the prediction varies with the length of the labeling interval. In general, relative differences between the measured urinary  $^{41}\text{Ca}/^{40}\text{Ca}$  isotope ratio and its predicted value were larger at day 180 when compared to those for day 90 of the assumed intervention period. As can be seen from Table 6, relative differences between measured and extrapolated  $^{41}\text{Ca}/^{40}\text{Ca}$  isotope ratios were larger when the run of the labeling curve was assessed by power law/exponential analysis techniques. This clearly shows that the compartmental modeling approach permits better prediction of the run of the labeling curve and, therefore, is preferable when attempting to identify the effect of an intervention on the urinary  $^{41}\text{Ca}$  signal. In any case, predicted  $^{41}\text{Ca}/^{40}\text{Ca}$  isotope ratios were significantly lower than the actual  $^{41}\text{Ca}/^{40}\text{Ca}$  isotope ratios in urine. Average offsets were on the order of 10% at day 90 of the intervention and 20% at day 180 using the compartmental

**Table 6** Identification of the predictive power of exponential/power law and compartmental modeling when used to describe urinary  $^{41}\text{Ca}$  excretion

Labeling period	Compartmental model		Exponential/power law model	
	90 days prediction	180 days prediction	90 days prediction	180 days prediction
200 days	$-4 \pm 7$	$-18 \pm 11$	$37 \pm 21$	$79 \pm 44$
300 days	$-14 \pm 8$	$-29 \pm 14$	$39 \pm 23$	$75 \pm 44$
400 days	$5 \pm 14$	$-12 \pm 16$	$14 \pm 21$	$4 \pm 35$
500 days	$-16 \pm 10$	$-20 \pm 6$	$35 \pm 40$	$40 \pm 42$

Labeling curves were modeled using the data obtained for subject subgroup A ( $n=6$ ) for assumed labeling intervals of 200, 300, 400 and 500 days, respectively. Curves were extrapolated to day 90 and day 180 as possible endpoints of a subsequent intervention. Data are presented as the relative differences in % of the measured from the calculated  $^{41}\text{Ca}/^{40}\text{Ca}$  isotope ratios around day 90 and day 180 from the end of the assumed labeling interval. Differences were calculated for the actual time points for which data were available ( $\pm 30$  days around day 90 and day 180 of the intervention interval) and grouped accordingly.

approach, and were even higher for the noncompartmental technique. Using compartmental modeling techniques, the between-subject variability of the offset (1 SD) was on the order of  $\pm 10\%$ , irrespective of the length of the labeling and the intervention period. This observation can be explained by imperfections in the underlying compartment model and small changes in Ca metabolism in the individual subjects that may have occurred over the observation period due to changes in diet, lifestyle or other factors.

The limitation of the approach described can be overcome by identifying induced changes in Ca transfer rates in the chosen compartment model itself. This can be done by including one or more additional fixed effect parameters  $\theta$  in the underlying equations describing the effect of the intervention on one (or more) transfer rates between compartments. As an example, Eq. 7 for the chosen three-compartment model must be modified as follows for an assumed effect of the intervention on the transfer rate  $k_{21}$  (see Fig. 3);  $\theta_7$  is an additional parameter describing the effect of the intervention on the transfer rate.

$$k_{21} = \theta_2 \cdot (1 - T \cdot \theta_7) \cdot e^{\eta_2} \quad (12)$$

A binary variable  $T$  must be included for computational reasons, to indicate the time point from which the effect becomes effective, i.e.,  $T=0$  during the labeling period and  $T=1$  during the intervention. Obviously, the transfer rates that are affected by the intervention are unknown a priori. A new model-finding procedure must be carried out in which all possible effects on the various transfer rates in the compartment model are tested in order to identify which of the modified models describe the experimental data best. Finally, a 95% confidence interval can be estimated for the additional parameter(s) using a likelihood ratio profile in order to explore whether the effect on one or more transfer rates is statistically significant [39]. Although this approach is more complex and requires extensive computing, model misspecifications are accounted for by using the same basic compartment model to evaluate data during the labeling

period as well as the intervention period. Furthermore, additional information is gained because the effects of the intervention on the individual Ca compartments can be assessed.

## Conclusion

We have successfully demonstrated that bone Ca can be labeled with the long-lived radioisotope  $^{41}\text{Ca}$ , and that urinary  $^{41}\text{Ca}$  excretion can be followed over periods of years using AMS, the most sensitive technique for isotopic analysis at the ultratrace level. RIMS, an alternative analytical approach to  $^{41}\text{Ca}$  analysis, is currently less sensitive and requires higher  $^{41}\text{Ca}$  enrichments/doses. However, this disadvantage is counterbalanced by its potential to make this technique more accessible to the research community. Although the RIMS instrument used is still a prototype and not commercially available, it is a tabletop instrument which can be manufactured at substantially lower costs than AMS. Using the series of certified  $^{41}\text{Ca}$  isotope reference materials produced especially for this application, it was possible to calibrate both techniques against each other [15], allowing the parallel use of both AMS and RIMS  $^{41}\text{Ca}$  analysis.

After administration of the isotope, it takes about 150–250 days until the maximum amount of tracer is incorporated into bone matrix. From this time point onward, the urinary  $^{41}\text{Ca}/^{40}\text{Ca}$  isotope ratio can be used to assess the effect of an intervention on bone. Using population compartmental modeling techniques, the urinary  $^{41}\text{Ca}$  excretion pattern can be described by a sequential three-compartmental model, which was found to be the preferred method/model for data evaluation. Besides giving a better description of urinary  $^{41}\text{Ca}$  excretion, it allows the effect of an intervention to be evaluated by identifying changes in transfer rates of the tracer.

This technique could potentially be used to evaluate the influence of diet and lifestyle on Ca metabolism in bone, and

to develop better strategies for osteoporosis prevention. The potential of the technique to assess the effect of interventions on bone health is currently under investigation.

**Acknowledgements** The authors would like to gratefully acknowledge all participants of the  $^{41}\text{Ca}$  workshop in Zurich (2004) and, in particular, Dr. Stewart Freeman for critical discussions. The authors would also like to thank Marlies Krähenbühl for her invaluable contributions in keeping the subjects motivated and her technical assistance. This work was carried out with financial support from the European Commission/Swiss Ministry of Science and Education (OSTEODIET, QLK1-CT 1999-000752; ETH Zurich/PSI, University of Mainz, Institute for Reference Materials and Measurements), from the U.S. Department of Energy through the University of California Lawrence Livermore National Laboratory under Contract No. W-7405-Eng-48, and from the Swiss National Science Foundation (Grant No.: 32-109352/1; University Hospital Bern).

## References

- Oeppen J, Vaupel JW (2002) *Science* 296:1029–1031
- Heaney RP (1998) *Endocrin Metab Clin* 27:255–265
- Compston JE, Papapoulos SE, Blanchard F (1998) *Osteoporos Int* 8:531–534
- Mazess RB, Barden HS, Bisek JP, Hanson J (1990) *Am J Clin Nutr* 51:1106–1112
- Genant HK, Faulkner KG, Gluer CC (1991) *Am J Med* 91:49S–53S
- Delmas PD, Beaudreuil J (1997) *Rev Rhum Engl Ed* 64:31S–36S
- Looker AC, Bauer DC, Chesnut CH, Gundberg CM, Hochberg MC, Klee G, Kleerekoper M, Watts NB, Bell NH (2000) *Osteoporos Int* 11:467–480
- Elmore D, Bhattacharyya MH, Saccogibson N, Peterson DP (1990) *Nucl Instrum Meth B* 52:531–535
- Wendt K, Blaum K, Bushaw BA, Juston F, Nortershauser W, Trautmann N, Wiche B (1997) *Fresenius J Anal Chem* 359:361–363
- Johnson RR, Berkovits D, Boaretto E, Gelbart Z, Ghelberg S, Meirav O, Paul M, Prior J, Sossi V, Venczel E (1994) *Nucl Instrum Meth B* 92:483–488
- Freeman S, Beck B, Bierman JM, Caffee MW, Heaney RP, Holloway L, Marcus R, Southon JR, Vogel JS (2000) *Nucl Instrum Meth B* 172:930–933
- Fitzgerald RL, Hillemonds DJ, Burton DW, Griffin TL, Mullaney S, Vogel JS, Defos LJ, Herold DA (2005) *Clin Chem* 51:2095–2102
- Carr TE, Harrison GE, Nolan J (1973) *Calcif Tissue Res* 12:217–226
- Weaver CM (1998) *Bone* 22:103S–104S
- Hennessy C, Berglund M, Ostermann M, Walczyk T, Synal H-A, Geppert C, Wendt K, Taylor PDP (2005) *Nucl Instrum Meth B* 229:281–292
- Hult MGJ, Johansson L, Johnston PN, Vasselli R (2003) *Environmental radiochemical analysis II*. Royal Society of Chemistry, Cambridge
- Hennessy C, Snell J, Quétel C (2003) Report of investigation into impurity levels in  $^{41}\text{Ca}$ -enriched material. IRMM, Geel
- Freeman S, Serfass RE, King JC, Southon JR, Fang Y, Woodhouse LR, Bench GS, McAninch JE (1995) *Nucl Instrum Meth B* 99:557–561
- Fink D, Middleton R, Klein J, Sharma P (1990) *Nucl Instrum Meth B* 47:79–96
- Hillemonds DJ, Fitzgerald R, Herold D, Lin Y, Vogel JS (2004) *J Assoc Lab Automat* 9:99–103
- Lin Y, Hillemonds DJ, Gertz ER, Van Loan MD, Vogel JS (2004) *Anal Biochem* 332:193–195
- Nishiizumi K, Caffee MW, DePaolo DJ (2000) *Nucl Instrum Meth B* 172:399–403
- Muller P, Bushaw BA, Blaum K, Diel S, Geppert C, Nahler A, Trautmann N, Nortershauser W, Wendt K (2001) *Fresenius J Anal Chem* 370:508–512
- Norris WP, Tyler SA, Brues AM (1958) *Science* 128:456–462
- Jung A, Bartholdi P, Mermillod B, Reeve J, Neer R (1978) *J Theor Biol* 73:131–157
- Heaney RP (1971) In: Bourne GH (ed) *Biochemistry and physiology of bone*, 2nd edn. Academic, New York
- Sheiner LB, Rosenberg B, Marathe VV (1977) *J Pharmacokinet Biopharm* 5:445–479
- Miller R (2001) In: Atkinson AJ (ed) *Principles of clinical pharmacology*. Academic, San Diego, CA
- Beal S, Sheiner L (eds)(1992) *NONMEM user guides*. NONMEM Project Group, Univ. of California at San Francisco, CA
- Fattinger KE, Sheiner LB, Verotta D (1995) *Biometrics* 51:1236–1251
- Sheiner LB (1984) *Drug Metab Rev* 15:153–171
- De Laeter JR, Bohlke JK, De Bièvre P, Hidaka H, Peiser HS, Rosman KJR, Taylor PDP (2003) *Pure Appl Chem* 75:683–800
- Robertson WG, Marshall RW (1981) *Crit Rev Clin Lab Sci* 15:85–125
- Nordin BE (1997) *Nutrition* 13:664–686
- Roth P, Hansen C, Werner E (1998) *Appl Radiat Isotopes* 49:687–689
- Wastney ME, Martin BR, Peacock M, Smith D, Jiang XY, Jackman LA, Weaver CM (2000) *J Clin Endocrinol Metab* 85:4470–4475
- Smith SM, Wastney ME, Morukov BV, Larina IM, Nyquist LE, Abrams SA, Taran EN, Shih CY, Nillen JL, Davis-Street JE, Rice BL, Lane HW (1999) *Am J Physiol* 277:R1–R10
- Neer R, Berman M, Fisher L, Rosenberg LE (1967) *J Clin Invest* 46:1364–1379
- Bates DM, Watts DG (eds) (1988) *Nonlinear regression analysis and its applications*. Wiley, New York